Comments on Inorganic Chemistry
Publication details, including instructions for authors and subscription information:
http://www.informaworld.com/smpp/title~content=t713455155

Application of NOE and PGSE NMR Methodologies to Investigate Non-Covalent Intimate Inorganic Adducts in Solution

Barbara Binotti[a]; Alceo Macchioni[b]; Cristiano Zuccaccia[b]; Daniele Zuccaccia[b]
[a] Istituto di Scienze Chimiche, University of Urbino, Urbino, Italy [b] Department of Chemistry, University of Perugia, Perugia, Italy

Online publication date: 14 September 2010

To cite this Article Binotti, Barbara , Macchioni, Alceo , Zuccaccia, Cristiano and Zuccaccia, Daniele(2002) 'Application of NOE and PGSE NMR Methodologies to Investigate Non-Covalent Intimate Inorganic Adducts in Solution', Comments on Inorganic Chemistry, 23: 6, 417 — 450
To link to this Article: DOI: 10.1080/02603590216079
URL: http://dx.doi.org/10.1080/02603590216079

Comments on Inorganic Chemistry, 23: 417–450, 2002

0260-3594/02 $12.00 + .00
DOI: 10.1080/02603590390163607

Application of NOE and PGSE NMR Methodologies to Investigate Non-Covalent Intimate Inorganic Adducts in Solution

Barbara Binotti
Istituto di Scienze Chimiche, University of Urbino,
Piazza Rinascimento, 6 – 61029 Urbino, Italy

Alceo Macchioni,* Cristiano Zuccaccia, and Daniele Zuccaccia
Department of Chemistry, University of Perugia,
Via Elce di Sotto, 8 – 06123 Perugia, Italy

NOE and PGSE NMR experiments provide crucial information for the structural characterization of non-covalent intimate adducts in solution. The possible presence and the favorite relative orientation of the interacting units can be deduced from NOE results, while the size of the non-covalent adducts can be estimated through PGSE measurements. The complementarity of the two methodologies has been successfully used to investigate transition metal complex ion pairs and, to a lesser extent, intermolecular adducts. The main results concerning the solution structures of non-covalent inorganic adducts are reported and compared with those in the solid state and those from theoretical calculations.

Keywords: NOESY and HOESY NMR, ion pairs, PGSE NMR, intermolecular adducts

INTRODUCTION

Weak interactions[1] are central to most chemical disciplines. They strongly affect the conformation and, consequently, the reactivity of biomolecules, the packing of solid materials, and the performances and stereodifferentiation of homogeneous catalysts.

*Corresponding author.

In coordination chemistry, weak interactions are even more important because their energy can be comparable to that of some coordinative bonds (for example X–H···M agostic bonds) and because the bonds involving a metal are usually easily polarizable. Consequently, in some cases, new types of weak interactions have been discovered such as the dihydrogen bond,[2] i.e., the hydrogen bond between X–H (X=O, N, etc...) and M–H (M = transition metal).

The methodologies for investigating weak interactions in the solid state are well-developed and rely mainly on X-ray diffraction studies.[3] In solution, some information can be obtained by "classical" techniques, but detailed insights into the presence and action of weak interactions can hardly be obtained especially for relatively small molecules. This is particularly true if the structure of the non-covalent assemblies, i.e., the relative position of the interacting moieties, has to be determined.

Recently it has been showed that NOE (Nuclear Overhauser Effect) NMR spectroscopies can be used successfully to investigate intermolecular adducts.[4] Initially, organic closed-shell ion pairs,[5] important for phase-transfer catalysis, and organolithium ion pairs[6] were the adducts taken into account. More recently, the NOE methodologies have been used to investigate the intermolecular structure of transition organometallic ion pairs,[7] cationic mono-organotin oxo clusters[8] and assemblies between neutral trinuclear Au(I) and Hg(II) units.[9]

Another basic bit of information that must be known is the size of the non-covalent adducts. This can be obtained by using the longstanding PGSE (Pulsed-Field Gradient Spin Echo) NMR methodologies.[10]

The combined information from the NOE and PGSE NMR methodologies usually provides a clear picture of the non-covalently bonded adducts in solution in that both the relative position of the interacting units and the nuclearity of the adducts can be determined.

In this paper, after having recalled the essential aspects of the NOE, Background and systems to be investigated, as well as PGSE measurements, the results of applying these techniques to transition metal complex ion pairs and neutral adducts are reported.

NMR METHODOLOGIES

Background of NOE

In diamagnetic systems in liquid phase, the most important source of relaxation for spin-1/2 nuclei is the nuclear dipole–dipole interaction. The Nuclear Overhauser Effect (NOE)[11] is a consequence of the dipole-dipole relaxation mechanism; for the simplest system consisting of two non-scalarly coupled spins, **I** (Interesting) and **S** (Saturated), separated by a constant distance (r_{IS}) and tumbling isotropically in solution, the steady-state NOE is

defined as the fractional enhancement of the signal of spin **I** under the continuous saturation of the resonance of the spin **S**:

$$\mathrm{NOE_I\{S\}} = \frac{\mathbf{I} - \mathbf{I}^0}{\mathbf{I}^0} = \frac{\gamma_S}{\gamma_I}\frac{W_{2IS} - W_{0IS}}{W_{2IS} + 2W_{1I} + W_{0IS}} = \frac{\gamma_S}{\gamma_I}\frac{\sigma_{IS}}{\rho_{IS}} \tag{1}$$

where I^0 is the equilibrium intensity of **I**, γ_S and γ_I are the gyromagnetic ratios of **I** and **S**, respectively, while W_{0IS}, W_{1I}, and W_{2IS} are the transition probabilities of zero-, single- and double-quantum pathways.[12] The term (W_{2IS}-W_{0IS}) represents the rate at which the NOE is transferred from **S** to **I** and is indicated by the symbol σ_{IS} (*cross-relaxation* rate constant). The quantity ($W_{2IS} + 2W_{1I} + W_{0IS}$) represents the *dipolar longitudinal relaxation* rate constant and is indicated with ρ_{IS}.[13] In the case of isotropic molecular tumbling, σ_{IS} and ρ_{IS} can be expressed as follows:

$$\sigma_{IS} = \left(\frac{\mu_0}{4\pi}\right)^2 \frac{\hbar^2\gamma_I^2\gamma_S^2}{10}\left(\frac{6\tau_C}{1 + (\omega_I + \omega_S)^2\tau_C^2} - \frac{\tau_C}{1 + (\omega_I - \omega_S)^2\tau_C^2}\right) r_{IS}^{-6} \tag{2}$$

$$\rho_{IS} = \left(\frac{\mu_0}{4\pi}\right)^2 \frac{\hbar^2\gamma_I^2\gamma_S^2}{10}\left(\frac{6\tau_C}{1 + (\omega_I + \omega_S)^2\tau_C^2} + \frac{3\tau_C}{1 + \omega_I^2\tau_C^2} - \frac{\tau_C}{1 + (\omega_I - \omega_S)^2\tau_C^2}\right) r_{IS}^{-6} \tag{3}$$

where μ_0 is the permeability constant in a vacuum, $\hbar$ is the Planck's constant divided by 2π, τ_c is the rotational correlation times, and ω_I and ω_S are the resonance frequencies of **I** and **S** nuclei, respectively. Both σ_{IS} and ρ_{IS} depend on the inverse of the sixth power of the internuclear distance and, therefore, the measurement of the steady-state NOE in this two simple spin system cannot be directly related to the internuclear distances.[14]

On the contrary, the measurement of the rate at which the NOE is transferred from **S** to **I** (kinetic of NOE build up), in our ideal two-spin system, allows σ_{IS} to be determined and, consequently, it can give direct information about the distance between **I** and **S**. In fact, the time course of the transient NOE experiments can be expressed by the following equation:

$$\mathrm{NOE_I\{S\}}(\tau_m) = e^{-(R - \sigma_{IS})\tau_m}\left(1 - e^{-2\sigma_{IS}\tau_m}\right) \tag{4}$$

where R represents the total longitudinal relaxation rate constants of both **I** and **S** spins, assumed to be equal, and τ_m is the mixing time. The first derivative with respect to the mixing time, at time zero, indicates that the initial build-up rate of the NOE is only proportional to σ_{IS}:

$$\left.\frac{d(\mathrm{NOE_I\{S\}})}{d\tau_m}\right|_{\tau_m=0} = 2\sigma_{IS} \tag{5}$$

In addition, at the early stage of the NOE build-up, all enhancements behave as if they were in a two-spin system approximation; σ_{IS} can be *quantitatively* derived (a) by limiting the NOE studies to the linear build up (Equation 5) of the **I** enhancement for short mixing times ($\tau_m \rightarrow 0$) or (b) by measuring the complete kinetics of NOE build-up and fitting the experimental data to Equation 4.[15]

Once σ_{IS} is known, the r_{IS} distance can be determined by Equation 2 after having evaluated the rotational correlation time, (τ_c), the other variable upon which σ depends. On the other hand, by comparing the σ_{IS} with that relative to two nuclei (**A** and **B**), whose internuclear distance is known (r_{AB} = calibration or reference distance[16]), an estimation of r_{IS} can be obtained by Equation 6 assuming that the proportionality constant between σ and r^{-6} is the same for the two couples of nuclei (**IS** and **AB**). For couples of nuclei having the same nature ($\gamma_I\gamma_S = \gamma_A\gamma_B$), this condition is satisfied when the rotational correlation times of the **I**-**S** and **A**-**B** vectors are equivalent.

$$\frac{\sigma_{IS}}{\sigma_{AB}} = \left(\frac{r_{IS}}{r_{AB}}\right)^{-6} \tag{6}$$

Suitable Systems to be Investigated

The above-illustrated essential features of the NOE should be sufficient for understanding which systems can be successfully investigated and what precautions must be taken. Some obvious requirements for the systems are (1) the presence of NMR active nuclei with high receptivity (H or F) in both moieties; and (2) the presence of magnetically non-equivalent nuclei, spatially dispersed around the interacting species, that will make it possible to discriminate different orientations inside the intermolecular adducts.

As we have seen in the previous paragraph, NOE strongly decreases with increasing r_{IS}. NOEs are usually classified as strong ($r_{IS} < 2.5$ Å), medium (2.5 Å $< r_{IS} <$ 3.3 Å), and weak ($r_{IS} > 3.3$ Å). The maximum distance at which NOE can be observed is ca. 5 Å, thereby introducing the limitation that only intimate adducts can be structurally investigated. Another limitation is caused by the presence of different types of internal motions that can change the actual value of both τ_c and r_{IS}. For instance, several motions in non covalently-bonded compounds could be present: (1) overall rotation of the adducts and/or the molecules constituting them; (2) adduct dissociation and formation; (3) internal motions (Me group rotations around single bonds and chair-boat inversion of the six-member cycles etc . . .). From the formal point of view, the presence of motions that are different from that of the overall isotropic molecular tumbling can be described by substituting in the Equations the above-reported σ_{IS}, r_{IS}^{-6}, and R with the corresponding mean values $\langle\sigma_{IS}\rangle$, $\langle r_{IS}^{-6}\rangle$, and $\langle R\rangle$. The type of expression that should be used to

determine the mean values depends on the rate of the motion that is active. The simplest situation occurs in the presence of internal motions that only change the actual value of τ_c without altering the internuclear distances. In this case, only motions that are faster than the overall motion contribute to the relaxation[17] but, at the same time, they cause the correlation function to drop rapidly to lower values, making the relaxation process less efficient.

Cases in which the internal motions change the actual values of both τ_c and r_{IS} are more complicated. When the motion is slower than the overall molecular tumbling, the corresponding effective distance "sensed" by the NOE is:

$$r_{effective} = \left(\frac{1}{N} \sum_{\mu=1}^{N} r_{IS,\mu}^{-6} \right)^{-\frac{1}{6}} \tag{7}$$

in which the index μ indicates the different conformations assumed by the spin system. In this case, in which we assume that all the conformations are equally populated, the average distances are underestimated by the NOE measurements. On the other hand, when the motion is faster than the molecular tumbling the effective distance is:[18,19]

$$r_{effective} \geq \left(\frac{1}{N} \sum_{\mu=1}^{N} r_{IS,\mu}^{-3} \right)^{-\frac{1}{3}} \tag{8}$$

in which the symbol " $\geq$ " is derived from the fact that the angular part of the correlation function can only reduce the size of the NOE. In this case, again assuming an equal distribution of the different conformations, the actual value of $r_{effective}$ (i.e., of the NOE) is determined by two factors: The average on the radial part tends to underestimate the "real" average value of r_{IS}, while the angular part, as discussed above, tends to reduce the NOE and, consequently, to overestimate the distance between **I** and **S**.

More complicated models have been proposed in the literature[20–24] that take into account the different distributions of the possible conformations; the conclusions are not at all consistent, but all the authors agree that the number of cases in which the internal motions would lead to significant error is fairly small. For the systems considered here, the molecular mass does not usually exceed 1000–1500 a.m.u. and the difference between the overall correlation time and the internal correlation time is less pronounced.

In any case, when the quantitative approach is needed, the assumption that the correlation time of the **I**, **S** and **A**, **B** pairs is the same must be verified.[25]

PGSE Measurements

Determining molecular self-diffusion coefficients by Pulsed Field Gradient Spin-Echo (PGSE) measurements[10] is a valuable methodology

for investigating the aggregation of molecular species in solution. Self-diffusion[26] is the net result of the thermal motion induced by random-walk processes experienced by particles or molecules in solution. In an isotropic homogeneous system the probability of finding a molecule, initially at position R_0, in a position R after a time t is:

$$P(R_0, R, t) = (4\pi Dt)^{-3/2} \cdot e^{-\frac{(R-R_0)^2}{4Dt}} \tag{9}$$

The single parameter D (self-diffusion coefficient) completely characterizes the spatial Gaussian distribution of the moving particle after a time t. Formally, the magnitude of the self-diffusion coefficient is given by:

$$D = \frac{k_b T}{f} \tag{10}$$

where T is the temperature, k_b is the Boltzmann constant, and f is the friction factor. For a rigid sphere of radius r in a continuous medium of viscosity, η_s, f is given by the Stokes equation:[27]

$$f = 6\pi\eta_S r \tag{11}$$

Combining Equation 10 and Equation 11 we obtain the Stokes-Einstein equation:

$$D = \frac{k_b T}{6\pi\eta_S r} \tag{12}$$

which relates the self-diffusion coefficient D to a molecular structural property, i.e., the hydrodynamic molecular radius (r). The latter and, consequently, the volume of the diffusing particles can be evaluated by knowing D. D can be measured by a number of NMR pulse sequences[10,28] based on the Spin-Echo sequence; the standard stimulated spin-echo sequence is shown in Figure 1.[10] By applying this sequence, the dependence

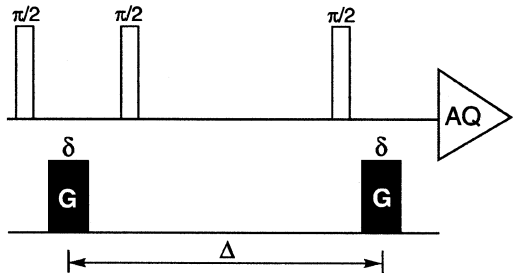

FIGURE 1 Standard stimulated spin-echo NMR pulses sequence.

of the resonance intensity (I) on a constant waiting time and on a varied gradient strength (G) is described by Equation 13:

$$\ln\frac{I}{I_0} = -(\gamma\delta)^2 D\left(\Delta - \frac{\delta}{3}\right)G^2 \tag{13}$$

where I is the intensity of the observed spin echo, I_0 is the intensity of the spin echo without gradients, D is the diffusion coefficient, Δ is the delay between the midpoints of the gradients, δ is the length of the gradient pulse, and γ is the magnetogyric ratio. The diffusion coefficient D is directly proportional to the slope of the regression line divided by Δ-$\delta/3$. In general, this is estimated by calibrating the experiments using the known diffusion coefficient of HDO in D_2O.[28]

The power of this technique is related to the useful information that can also be obtained for complicated mixtures. As long as the different components have at least one resonance that is clearly resolved in the spectrum, the various diffusion coefficients can be determined from a single experiment. In those cases in which there are no resolved resonances for the components in the proton spectrum, some information can be gained by (a) taking into account different nuclei like ^{19}F or ^{31}P or (b) combining the diffusion sequences with different spectral filtering techniques such as X filtering[29] or with 2D correlation experiments and PGSE technique.[28]

It can be argued that the PGSE methodologies appear simple and, in general, can be applied in a straightforward way. On the other hand, the results can be very precise but not at all accurate, due to the presence of different sources of possible errors. The inaccuracy can come from convection currents (mass convection) when solvents with low viscosity are used. In this case it is advisable to repeat the experiment using different diffusion periods (Δ)[30a,30c] to check the reproducibility of the results. Alternatively, more complicated sequences are available to reduce the effect of convection, but these have a low sensitivity.[31] Another source of inaccuracy can be derived from changes in solution viscosity when the dependence of the diffusion coefficients (and so the aggregation size) on the concentration needs to be known. In such cases, it is highly advisable to use an internal standard (preferably with a volume and shape similar to one component of the system being investigated).[30a,30b,32]

RELATIVE ANION-CATION POSITION IN IONIC COMPLEXES

The interionic structure of the complexes illustrated in Scheme 1 and Scheme 2 have been investigated through ^{1}H-NOESY and ^{19}F,^{1}H-HOESY NMR experiments in solvents (methylene chloride or chloroform) and at concentrations (10^{-2}—10^{-1} M) that ensure the predominance of intimate ion pairs. The results from the qualitative investigations are considered in the

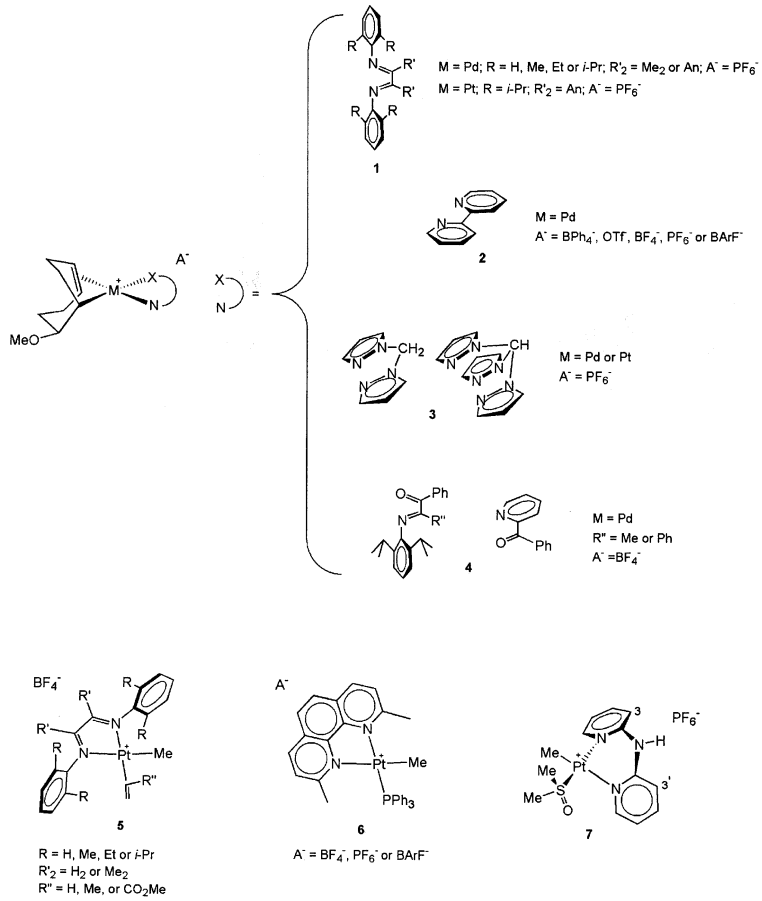

SCHEME 1

section on quantitative investigation where they are organized according to the nature of the N,X ligand and to the geometry of the metal center. The relationships between the solution interionic structure (from the qualitative NOE NMR investigation), the structural data in the solid state and the results of theoretical calculations are outlined. The results from the quantification of the interionic NOEs and, consequently, the estimation of average interionic distances are illustrated in the section on qualitative investigation. The **10a** compounds were considered because they contain unsymmetrical counter-anions and show not only a specific localization but also a specific orientation of the anion.

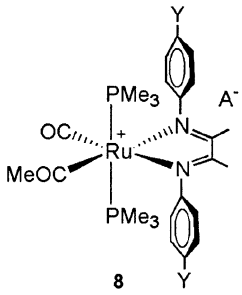

8

Y = H or F
A^- = BPh_4^- or BF_4^-

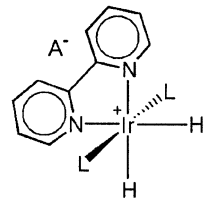

9

L = PPh_3 or PPh_2Me
A^- = BPh_4^-, OTf^-, BF_4^- or PF_6^-

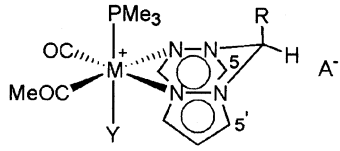

10

M = Fe, Ru or Os; R = H or pz; Y = PMe_3, CO or pz; A^- = BPh_4^-, OTf^-, BF_4^- or PF_6^-
M = Ru; R = H; A^- = $BR'Ph_3^-$; R' = Me, *n*-Bu, *n*-Hex or Ph (**10a**)

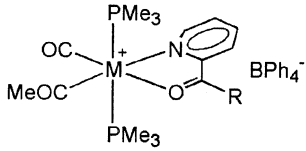

11

M = Fe or Ru
R = Me, Ph or pz

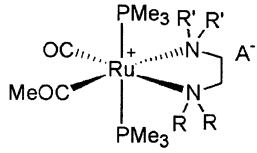

12

R = H, Me or bz
R' = H, Me, Et, *i*-Pr or bz
A^- = BPh_4^-, BF_4^- or PF_6^-

SCHEME 2

Qualitative NOE NMR Investigations

α-*Diimine Ligands*

1,4-diaza-1,3-butadiene derivatives (α-diimines) have attracted much interest because of their versatile coordination behavior and the interesting properties of their metal complexes.[33] 1,4-disubstituted 1,4-diaza-1,3-butadienes, RN=CR′–CR′=NR are the simplest representatives of this class of compounds. They are particularly fascinating because they have a flexible N=C–C=N skeleton, they appear to have unusual electron-donor and -acceptor properties and can potentially act in a variety of coordination modes. The latter bonding modes involve not only the lone pairs of the N atom but also the π–C=N bonds. Of course, factors such as the R and R′ substituents, the metal atom and other ligands bonded to the metal influence the type of coordination of the 1,4-diaza-1,3-butadienes. The chemistry and structural aspects of metal complexes containing chelated bonded RN=CR′–CR′=NR ligands have been well explored; this is probably due to the possibility of easily tuning the electronic and steric properties by changing both the R and R′ substituents. For these reasons, α-diimines have been used successfully as support ligands for nickel and palladium catalyst systems for polymerizing ethylene, α-olefins and cyclic olefins and copolymerizing non-polar olefins with a variety of functionalized olefins.[34] In such catalysts, R is very often an aryl group having hindered *ortho*-substituents.

Olefin platinum(II) and palladium(II) complex ion pairs. With the principal aim of investigating whether the anion-cation interactions could afford useful information for understanding some catalytic features, complexes **1**[35] and **5**[36] were considered. Complexes **1** are good catalysts for the CO/styrene copolymerization carried out in mild conditions, whereas complexes **5** are analogous to the resting state of the Brookhart's catalysts for the polymerization of α-olefins.[34]

All complexes **5** show very strong interionic contacts between the fluorine atoms of BF_4^- and the protons of the R′ groups; there are also strong interionic contacts with the protons of some R substituents. When R = *i*–Pr, all eight isopropyl methyl groups are magnetically non-equivalent due to a restricted rotation around the C–N bond, and only the ones pointing toward the R′ substituents show interionic interactions with BF_4^-. Since the steric hindrance above and below the coordination plane introduced by the N,N-diimine ligands decreases (R < Et for **5** having R″ = Me; R < *i*–Pr for **5** having R″ = H), weak interionic contacts with the Pt–Me, R″ and olefinic protons start to appear (Figure 2). Such results indicate that the counterion pairs with the organometallic fragment on the side of the N,N-ligand, preferentially interacting with the R′ and R groups. Furthermore, its exact position is tuned by the steric hindrance of R, R′ and R″. As the steric

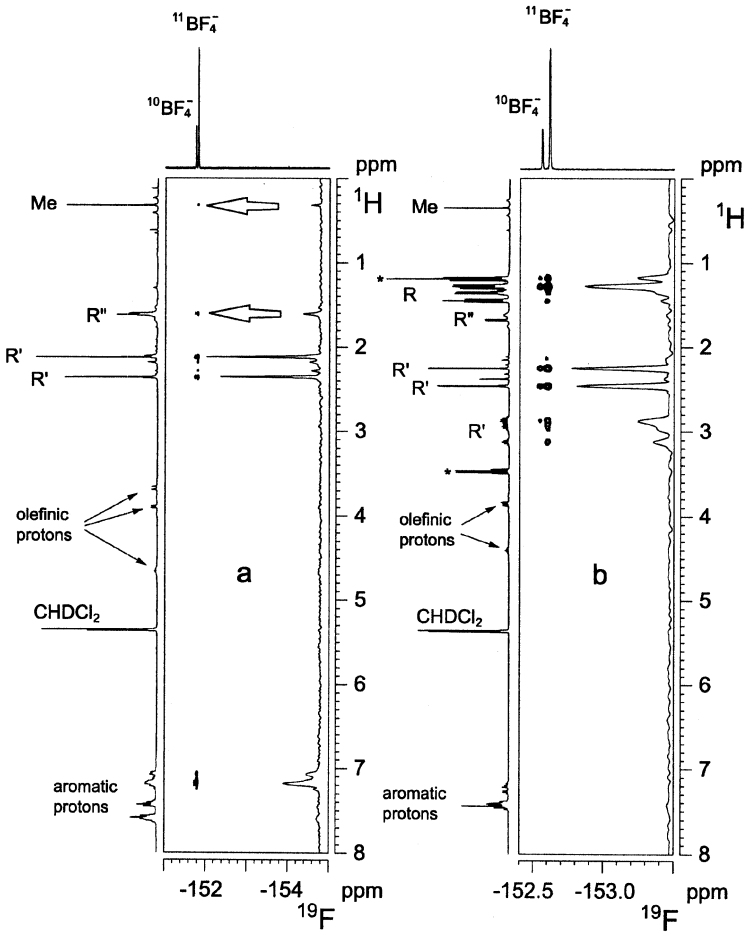

FIGURE 2 The two ^{19}F, ^1H-HOESY NMR spectra (376.65 MHz, 298 K, methylene chloride-d_2, $\tau_m = 0.8$ s) show the disappearance of interionic interactions between BF_4^- and Me–Pt and R″ (indicated with arrows) going from R = H (a) to R = *i*–Pr (b). The F1-trace (indirect dimension) relative to one component of fluorine doublet is reported on the right of every spectrum. * indicates the resonances of a little impurity of OEt_2. Reproduced from Ref. 7 with the permission of the *European Journal of Inorganic Chemistry*.

hindrance decreases, the counterion populates positions closer to the platinum even if it is still substantially shifted toward the nitrogen ligands. In agreement with our findings for these platinum complexes, Tilset et al.[37] showed by means of DFT calculations, that the association of solvent molecules, such as water or trifluoroethanol, with the cationic σ-complexes $[(\alpha\text{-diimine})PtMe(CH_4)]^+$ occurs at the C–C diimine bond where the positive charge accumulates.

The investigation of the interionic solution structure of complex ion pairs **1** afforded results that were similar to those of the above-discussed platinum compounds. In the series in which $R'_2 = Me_2$ and R spans from H to *i*–Pr, PF_6^- interacts preferentially with R′ and R protons. In the platinum complexes **5** the access to the metal center was completely inhibited when $R \geq Et$; in this case we found that the metal was completely protected when $R = Me$.[35] This could be due to greater accumulation of positive charge in these palladium complexes with respect to the **5** platinum compounds. This accumulation was induced by the higher *trans* effect of the carbon σ-bonded to Pd with respect to Me and/or to a higher apical steric hindrance of the cyclo-octenylmethoxy-moiety with respect to the olefin substituents of the Pt complexes. This point indicates that the steric hindrance in the axial sites was additive among all the ligands coordinated to the metal. The results for complexes where $R'_2 = An$ (9-Anthryl) and $R = i$–Pr were even more interesting. In this case the steric protection did not guarantee a specific interionic structure; PF_6^- interacted with several protons including those belonging to the cyclo-octenylmethoxy moiety, and the observed dipolar interactions could not be explained by the predominance of only one structure of ion pair. The loss of specificity could be due to the difficulty that the counterion has in approaching the diiminic carbons, because they are sterically protected by the An-substituents, or to a general wider dispersion of the cationic charge.

Acetyl ruthenium(II) complexes. The interionic structure of octahedral complexes bearing α-diimines analogous to those shown above was also studied. In such cases, the apical positions are occupied by two ligands and only α-diimines with small ortho-substituents can be used.

In particular, complexes **8**[38] (Scheme 2) were synthesized. The counteranion preferentially resides on the side of the diimine ligand above or below the plane defined by the N, N, CO, and COMe ligands. The ^{1}H-NOESY NMR spectrum of the compound where $A^- = BPh_4^-$ shows that the phosphine protons interact quite strongly with all the aromatic protons of the anion, while the methyl groups of the diimine ligand interact with its *ortho* and *meta* protons. The interactions between the counterion and the aromatic protons of the cation can be detected more readily in the ^{19}F,^{1}H-HOESY NMR spectra of compounds containing BF_4^-. No contacts were detected between the anion and the COMe protons or *p*-H or *p*-F in any complex.

Bipyridine and Phenanthroline Ligands

Bipyridines, phenantrolines and their various derivatives are some of the most widely used ligands in chemistry. Currently, bipyridine derivatives figure prominently in supramolecular chemistry, conformationally constrained peptides, sensors and receptors, polymer chemistry, studies of redox electrocatalysis, electron transfer, photochemistry, electroluminescence, and a variety of other fields.[39] Furthermore, both the 2,2′-bipyridine and 1,10-phenanthroline ligands have been extensively used as metal chelating ligands in the alternating copolymerization of carbon monoxide and styrene or ethene.[40]

Palladium(II) and platinum(II) complexes. In compounds **2**[41] the anion is located in the expected position above and below the square planar coordination plane due to the absence of steric hindrance or electronic protection in such positions. The two axial sites are preferred and are equally populated by the counterion even if it is slightly shifted toward the pyridine ring *trans* to the Pd–C σ-bond (Figure 3). This takes place regardless of the A^- nature, while the intensity of the interionic NOEs decreases as the coordinating tendency decreases: $CF_3SO_3^- > BF_4^- > PF_6^- > B(3,5\text{-}(CF_3)_2C_6H_3)_4^-$. This interionic structure in solution differs from that observed in the solid state for the complex containing the PF_6^- anion. In the solid state, the counteranions are lined up located sideways around the coordination plane while the cationic moieties are stacked. The shortest contacts between

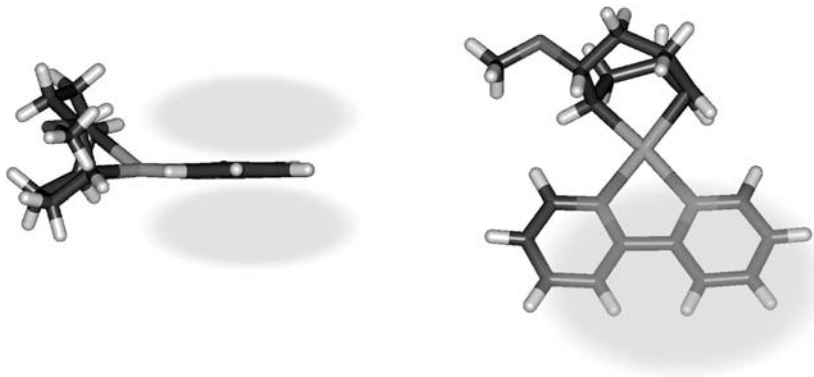

FIGURE 3 Two views of the solution interionic structure of [Pd(η^1,η^2-C_8H_{12}OMe)-(bipy)]A complexes where the gray clouds represent the action space of the A^- counteranion. The two positions above and below the coordination plane are equally populated and the anion is shifted on the side of bipy ligand with a slight preference for the ring *trans* to the Pd–C σ bond. Reproduced from Ref. 7 with the permission of the *European Journal of Inorganic Chemistry*.

the fluorine and the complex hydrogen atoms are about 2.5 Å. Moreover, no interaction between the metal and the anion was observed, which means that packing forces in the solid state are predominant over Pd · · · F interactions.

The cationic methyl platinum(II) complexes **6**[42] bearing the 2,9-dimethyl-1,10-phenanthroline (dmphen) ligand, are an example of reduced anion-cation interaction specificity.[19]F,[1]H-HOESY NMR spectra of these compounds show intense crosspeaks between the fluorine atoms of the PF_6^- or BF_4^- counterions and all the aromatic protons, even if the contacts with PPh_3 protons are weaker. There are also weak contacts with the methyl substituents of the dmphen ligand. However, no contact was observed with the methyl group directly bonded to the platinum. From these results it can be deduced that, in solution, the anion stays on the side of the phenanthroline ligand, in agreement with what was found in the solid-state for the compound bearing the PF_6^- anion. In contrast to complexes **2** illustrated above, which contain the planar "non-hindered" bipyridine ligand, in such tetrahedral distorted square planar complexes the positions above and below the coordination plane are different. The counterion prefers a location below the aromatic rings of the phenanthroline but the situation is not static and it still has the possibility to oscillate up and down, interacting weakly with the phosphine hydrogen atoms (Figure 4).

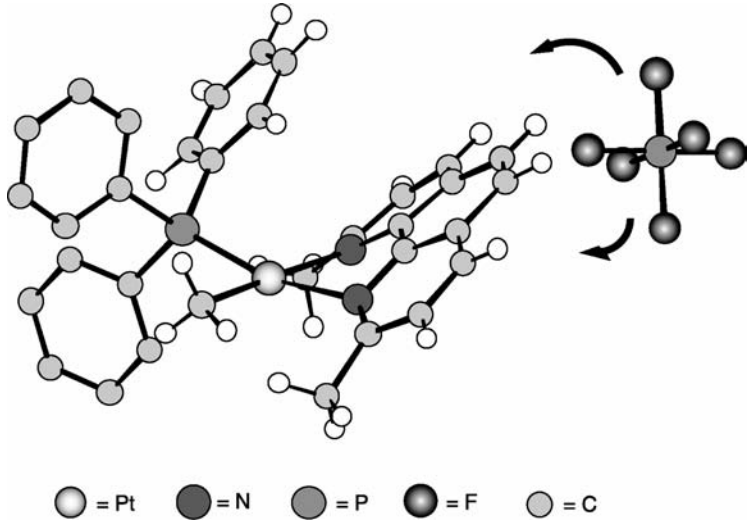

FIGURE 4 Balls and sticks schematization of the ion-pair solution structure of **6**. The structural parameters for the two ionic moieties were obtained from X-ray data. Reproduced from Ref. 42 with the permission of the American Chemical Society.

Octahedral iridium(III) complexes. In complexes **9**[43], the anion would have the apparently favorable possibility of binding near the IrH_2 group, which would give the closest Ir-anion distance and allow hydrogen bonding.[44] Instead, the anion is specifically located near to the bipy ligand interacting with 3 (strong), 4 (medium), 5 (weak) and phosphine protons (Scheme 3); the interaction specificity falls off with increasing anion size. In perfect agreement with $^{19}F,^{1}H$-HOESY NMR results, natural population analysis (NPA)[45] on the optimized geometry of the cation identify the predominant location of the positive charge at the bipyridyl ring carbons that take part in the inter-ring C–C bond. The electrostatic potential calculated for the cation confirms the location of the preferred binding site. In contrast, in the solid state the counteranion is found close to one of the hydrides and close to proton H-6 and H-5 of one of the pyridines, and this fact suggests that the solid-state structure might then be a compromise between this preferred geometry of ion pair and a more compact and more stable packing in the solid state. Pregosin et al.[46] recently reported that also in several Ir(III) dihydrido-complexes bearing P,N-ligands the anion did not interact with hydrides and was located close to the N-arm.

Poly(pyrazol-1-yl)methane and Bis(2-pyridyl)amine Ligands

The poly(pyrazol-1-yl)methane ligands are formally derived from the extensively studied poly(pyrazol-1-yl)borate[47] ligands by replacing a boron anion with a carbon atom and are, thus, isoelectronic to them. Jordan, Canty

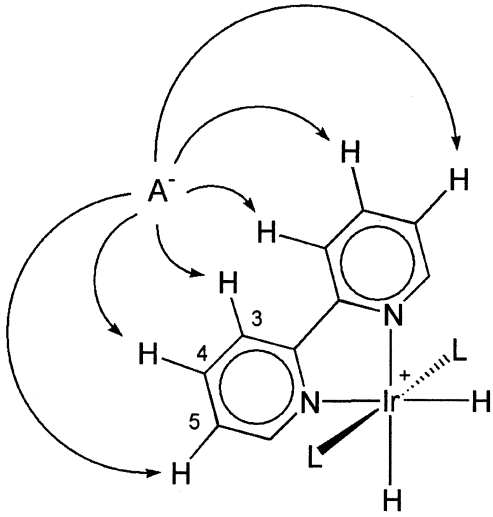

SCHEME 3

et al. have prepared several types of neutral and cationic Pd(II) complexes incorporating bis(pyrazol-1-yl)methane ligands, including $[\{(R_2C(pz)_2)\}$-$PdMe(L)]^+$ where L is a labile ligand or substrate.[48] The neutral nitrogen bidentate ligand forms six-membered-boat metallacycles when chelating a palladium metal atom and this boat conformation may undergo inversion, which results in an exchange between the axial and equatorial CR_2 substituents. Pyrazoles are weaker σ-donors than imine or pyridine ligands, and therefore the palladium cations bearing such ligands may be more electrophylic.[48] The tris(pyrazol-1-yl)methane or tris(pyrazol-1-yl)borate ligands are usually found as trihapto donors in octahedral complexes; otherwise, they behave like dihapto donors in square planar complexes according to the electronic requirements of the metal centers.[49]

In the bis(2-pyridyl)amine (dpa) ligand the presence of a spacer group between the pyridine rings is expected to produce remarkable differences in the properties of complexes containing the bipy or the dpa. Upon coordination to a metal in a square planar configuration, this ligand forms a nonplanar six-membered ring in analogy with poly(pyrazol-1-yl)-methanes.[50] In platinum(II) complexes, the lack of planarity and the loss of aromatization of ancillary ligands lead to a reduced reactivity.[51]

Square planar platinum(II) and palladium(II) complexes. In complexes **3**[52] containing the nonplanar bis- and tris(pyrazol-1-yl)-methane ligands there is a remarkable specificity in the interaction between the cation and the anion that is incredibly higher than that observed in similar compounds where the N,N-ligand is planar (complexes **2**). In fact, while in the latter compounds the anion interacts preferentially with the protons belonging to the bipy ligand (as described in the section on pt(II) and pd(II) complexes) but still sees the protons belonging to the cyclooctenyl moiety that are closer to the metal, in complexes **3**, the PF_6^- interacts exclusively with the peripheral protons of the nitrogen ligands (Figure 5).

The interionic structure of the five-coordinate complexes can be rationalized by using considerations similar to those valid for octahedral compounds. In compounds bearing the bis(pyrazol-1-yl)methane ligands, the apical positions are only partially protected by the steric hindrance introduced by the boat conformation of the MNNCNN cycle and the PF_6^- should be able to occupy the non-hindered apical positions. Instead, it prefers to locate in the peripheral part of the N,N-ligand. The reason for such unexpected specificity has to be found in the formation of a F···H weak hydrogen bond between the $H_2C(N)_2$ moiety and an F-atom of the counterion that provides an electronic protection of the metal center. All the spectroscopic evidence agrees with the identification of a specific ion pair for the palladium five-coordinate complex in the crystalline state, stabilized by an assembly of hydrogen bonds within the ion pair, with the strongest interactions involving the highly polarized $H–C(N)_3$ proton and fluorine lone pairs. The anion-cation recognition is very specific; the space-filling representation of the ion

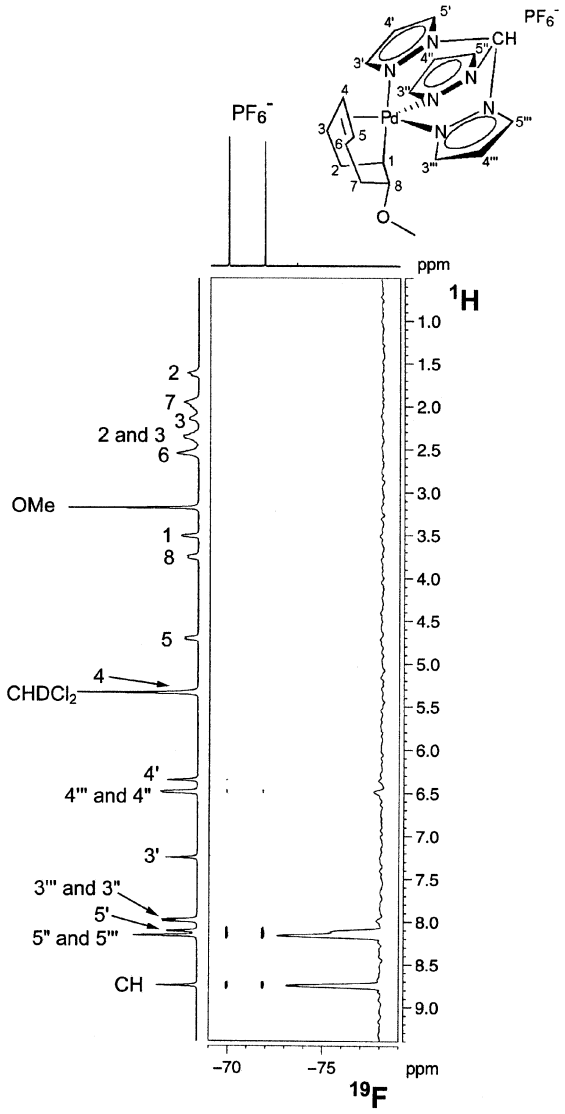

FIGURE 5 ^{19}F, ^{1}H-HOESY NMR spectrum (376.65 MHz, 188 K, methylene chloride-d_2, $\tau_m = 0.8$ s) of compound $[Pd(\eta^1,\eta^2\text{-}C_8H_{12}OMe)\{(pz_3)CH\}]PF_6$ showing the remarkable specificity of the interaction between PF_6^- and the 5′-5‴ and 4′-4‴ (very weak) protons of the cation. The 1D-trace relative to the PF_6^- column is reported on the right. Reproduced from Ref. 52 with the permission of the American Chemical Society.

pair clearly shows the cation pocket where the anion fits in a sort of docking process (Figure 6).

Clear electronic protection of the apical positions was also encountered in investigating the cationic Pt(II) complex **7**[53] containing the bis(2-pyridyl)-amine (dpa) ligand. The $^{19}F,^{1}H$-HOESY NMR spectra showed strong interionic contacts between the fluorine atoms of the counterion and the bridging N–H, H3, and H3′ protons of the nitrogen ligand (Scheme 1) and a weak interaction with the dimethyl sulfoxide protons. This means that the preferential position of the counterion is close to the amine N–H proton of the nonplanar six-membered ring formed by the dpa coordinated to the metal. Furthermore, the interaction of PF_6^- with the acid N–H proton makes the atoms of fluorine unequivalent, affording a 1:4:1 signal, so the ^{19}F NMR spectrum appears as an apparently structured doublet. The most reasonable explanation of this finding is the formation of $NH\cdots FPF_5^-$ hydrogen bonds that again provide an electronic protection of the metal center. This averaged interionic solution structure is similar to that observed in the solid state for the analogous complex containing the $CF_3SO_3^-$ anion, where the presence of a strong hydrogen bonding interaction between the amine hydrogen and the triflate anion oxygen was clearly detected.

Octahedral complexes. The interionic structure of **10** in which the counterion was BPh_4^- was investigated first.[54,55] The interionic contacts, between the *ortho* protons of the anion and the 5 and CHR protons (medium)

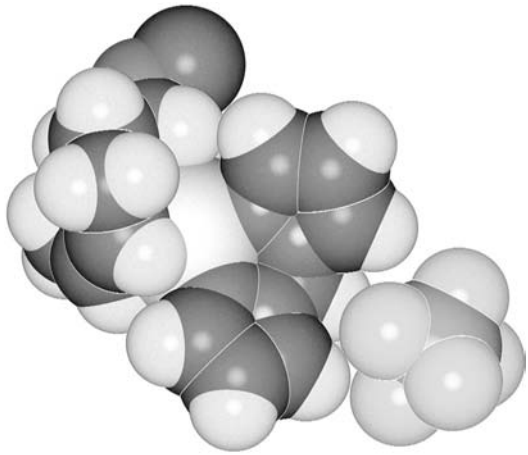

FIGURE 6 Space-filling diagram of the palladium complex **3** bearing the tris(pyrazol-1-yl)methane ligand. Reproduced from Ref. 52 with the permission of the American Chemical Society.

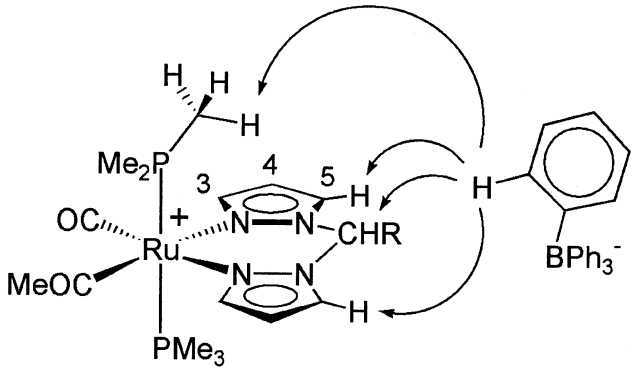

SCHEME 4

of the cation and the phosphine protons (weak), observed in the ^{1}H-NOESY NMR spectra, and the absence of interactions with the COMe protons, led to the conclusion that the anion is specifically located close to the bispyrazolyl-ligand (Scheme 4). The same relative anion-cation orientation was found in ^{19}F,^{1}H-HOESY NMR studies using fluorinated counterions (BF_4^-, PF_6^- and $CF_3SO_3^-$). The solid state data of compound *cis*-[Ru(COMe){$(pz_2)CH_2$}$(CO)_2(PMe_3)$]BPh_4[56] shows that the cation is surrounded by six symmetry-related anions. Quantum mechanic and mechanical docking calculations[56] on the solid state data show that the ion pairs where the counterion orients two of its phenyl group almost parallel to the pyrazolyl rings is favorite (Figure 7). These results perfectly match the interionic structure observed in solution. From the above-mentioned theoretical calculations, there is an accumulation of positive charge at the CHR carbon, while the negative charge is concentrated on the oxygen of the COMe group. The ion pair with the counteranion on the side of the pyrazolyl-rings is,

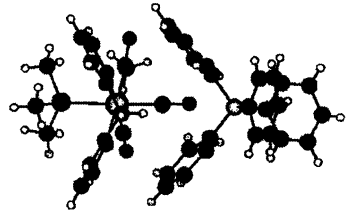

FIGURE 7 Solid state structure of *cis*-[Ru(COMe){$(pz_2)CH_2$}$(CO)_2(PMe_3)$]BPh_4 where the notably shortest Ru···B metal contact is found. Reproduced from Ref. 56 with the permission of the American Chemical Society.

consequently, dictated by a gain in the electrostatic interaction energy. When BPh_4^- is taken into account, the observed relative anion-cation position is further stabilized by the favorable lipophilic interactions between the phenyl groups of the anion and the pyrazolyl-rings. These π-stacking interactions lead to an energy gain of about $4\,kJ/mol$[57] and could compensate for the reduction of favorable Coulomb interactions due to an increase in the average anion-cation distance going from BF_4^- or PF_6^- to BPh_4^-.

α-Diamine Ligands

Compounds incorporating the 1,2-diamine functionality are currently being studied in several fields.[58] In particular, chiral, enantiomerically pure 1,2-diamine, and their derivatives are increasingly being used in stereoselective organic synthesis; for example, as chiral auxiliaries, or as metal ligands in catalytic asymmetric synthesis, as in the catalytic asymmetric hydride transfer reduction of ketones.[59]

Octahedral ruthenium(II) complexes. Ruthenium(II) compounds bearing substituted ethylenediamines (**12**)[38] were investigated in order to determine if the high specificity in the anion-cation interactions was confined to the presence of N-aromatic ligands. A section of the ^{1}H-NOESY NMR spectra, relative to the simplest compound taken into account, is reported in Figure 8. The intensity of the interionic interactions between the anion and the protons of the ethylendiamine decreases by moving from NH_2^d to NH_2^a. In the absence of conjugation, the anion is still located close to the N,N-ligand; it even prefers the N-arm *trans* to the COMe group, where the electron density is reduced due to the high *trans* influence of COMe. The introduction of steric hindrance in the N,N-ligand (by using $NRHCH_2CH_2NR'H$ ligands) affords a fine modulation of the anion position that shifts toward less crowded "places." For example, when $R = R' = CH_2C_6H_5$ (bz), two stereoisomers are present, depending on the orientation of the bz-groups with respect to the phosphines. In the stereoisomer having the two bz-groups oriented toward the same phosphine, the anion stays close to the N,N-ligand but preferentially interacts with the protons of the other phosphine group.

N,O-Ligands

In recent years, coordination chemistry of chelated ligands containing mixed functionalities on transition metal centers has been an extremely active area of research. In particular, the chemistry of hemilabile ligands[60], which contain both substitutionally inert and substitutionally labile groups, has received considerable attention. These ligands are polydentate chelates that contain at least two different types of bonding groups: one group bonds strongly to a metal center, while the other bonds weakly and is therefore easily displaced by coordinating ligands or solvent molecules. This

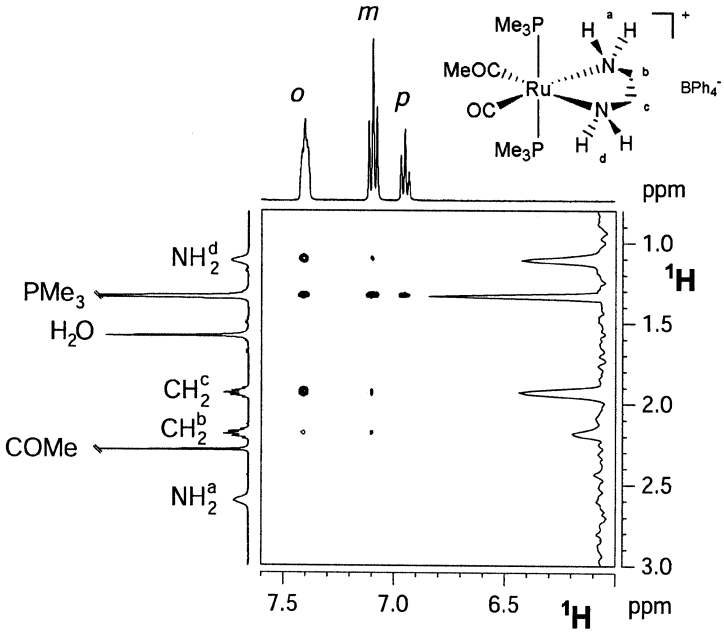

FIGURE 8 A section of the ^{1}H-NOESY NMR spectrum of the illustrated complex showing the gradual decrease of the interionic contact intensity passing from positions d to a. The 1D-trace relative to the *ortho* proton column is reported on the right (400.13 MHz, 298 K, methylene chloride-d_2, $\tau_m = 0.8$ s). Reproduced from Ref. 61 with the permission of the *European Journal of Inorganic Chemistry*.

displacement reaction can be a reversible process. The bifunctional character of hemilabile ligands has been shown to be useful in homogeneous transition metal catalysis, metal complex small molecule activation, chemical sensing, and the stabilization of reactive, unsaturated transition metal species. In particular, when cationic transition metal complexes are considered, the anion and the labile arm can compete for occupancy of the coordination site.

Olefin Pd(II) complexes containing α-Iminoketone ligands. In the cationic Pd(II) complexes **4**[61] the anion, remaining on the side of the neutral N,O-ligands, has the possibility of choosing the least crowded side close to the O-arm or the electronically favored position close to the imine carbon. The observed interionic structure suggests that both positions are present in solution in almost the same abundance. An X-ray structural study carried out on the complex where R″ = Ph showed that the interionic solid state structure is more specific than that observed in solution. Interestingly,

the first of the nearest neighbor anions surrounding the cation is located on its less encumbered site, i.e., close to the O-arm of the hemi-hindered α-iminoketone N,O-ligand.

Cationic acetyl complexes of Fe(II) and Ru(II). The interionic structure of complexes **12**[62] bearing neutral N,O-ligands, investigated in CD_2Cl_2 by the NOESY NMR spectroscopy, indicated that, for all complexes, BPh_4^- is specifically localized in front of the face determined by PMe_3 and both arms of the N,O-ligands. A confirmation of the specificity of the contacts is that we never observed dipolar interactions between the counterion and M–COMe protons. The interionic structure of the ruthenium complex bearing the 2-benzoylpyridine ligand determined by single-crystal X-ray studies presents the counterion between the CO and O-arm of the N,O-ligand. This means that the anion position is slightly different than that found in solution where we also observed contacts between *ortho* protons of BPh_4^- and protons belonging to the pyridyl ring (Scheme 5).

Conclusions for Qualitative NOE NMR Investigations

From the investigations on transition metal complex ion pairs, some general features can be derived. The anion has a strong tendency to locate close to the nitrogen-based ligand independent of its nature and that of the solvent, both in cases with unsaturated and saturated N,X-ligands. There are two conditions that allow a well-defined anion-cation relative position: (1) electron polarizability of the complex that causes an accumulation of positive charge far away from the metal, on the side of nitrogen-based ligands; and (2) axial steric and/or electronic protection of the metal. The second condition is naturally reached in octahedral complexes where the ion-pair structure is, consequently, determined by (1). In the case of square planar complexes, the apparently favored apical positions for the anion are often protected due to electronic factors or to a mix of electronic and steric factors. Furthermore, the

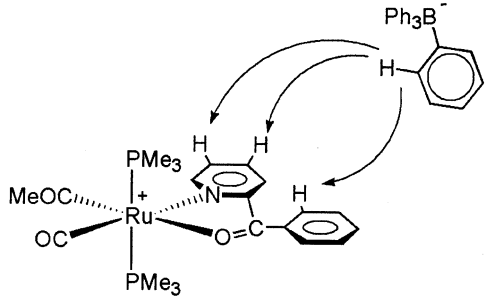

SCHEME 5

anion accessibility to the metal center appears to be finely modulated by the steric hindrance in the apical positions.

The structure of ion pairs has sometimes been inferred from X-ray structural work where it was assumed that the solution structure, the only structure relevant to reactivity in solution, was the same as in the solid. The results obtained in our investigations suggest that the surprisingly well-defined structures in solution are often broadly similar to the solid-state structure. For example, in one case the cation is surrounded in the solid state by six symmetry-related anions, only one of which reflects the solution structure. In such a case, even with the solid (octahedral complexes) state structure in hand, it would not be obvious which of the ion pairs seen in the solid resembles the solution structure.

Furthermore, we show how theoretical calculations can satisfactorily explain the ion pair structure found in solution. The electron density on both ionic fragments and the energy interaction values of the ion pairs evaluated by quantum mechanic calculations (see sections on iridium and octahedral complexes) are consistent with the experimental results and confirm the location of the preferred binding site.

Quantitative NMR Investigation for Complexes Bearing Unsymmetrical Counterions

According to what was stated in paragraph 1, average interionic distances can be estimated by the quantification of the NOEs. We started our investigations with **10a** complexes.[25] From qualitative ^{1}H-NOESY NMR studies, we knew that the anion orients two phenyl rings almost parallel to the two pz-rings and the aliphatic chain (R = *n*-Bu or *n*-Hex) distant from the metal center (see octahedral complexes section).[63] When R = Me the qualitative approach did not give a definitive answer because both B–Me and *ortho* protons interacted with the CH_2 and H5 protons of the cationic moiety. We then decided to quantify the NOEs by recording the kinetics of NOE build-up by inverting several target resonances using the *selno* (*se*lective *no*esy)[64,65] and *selnogp* (*se*lective *no*esy with field *g*radient *p*ulses)[66,67] NMR pulse sequences. An example of intramolecular and interionic NOE build-up is showed in Figure 9. Average interionic distances were estimated by taking the *o*H–*m*H distance (2.47 Å) as a reference. In order to check the accuracy of the determined average interionic distances, rotational correlation times were estimated by using two independent NMR methodologies: ^{13}C relaxation measurements[68–70] and the dependence of the ^{1}H–^{1}H cross relaxation on the temperature. With both methodologies, it was found that intramolecular and interionic couples of nuclei have the same rotational correlation times (ca. 100 ps) within the experimental error and are about 3.8 times higher than those related to couples of nuclei belonging to *trans*-Ru(COMe){$(pz_2)BH_2$}(CO)$(PMe_3)_2$. The latter compound[71] is

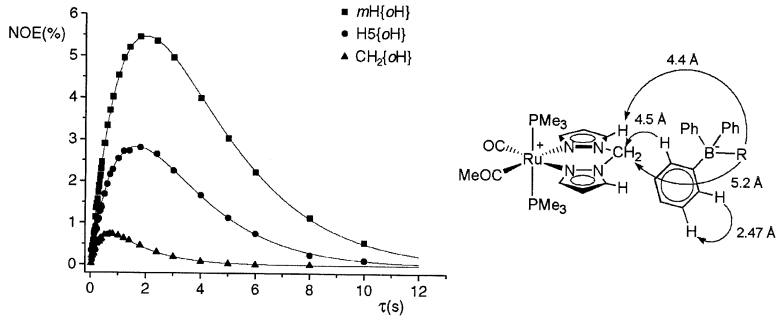

FIGURE 9 Experimental data relative to the %NOE as a function of τ for the irradiation of *o*H protons of the BPh_4^- (T = 302 K) for complex in which R = Ph. Reproduced from Ref. 25 with the permission of the American Chemical Society.

isosteric and almost isomass with the cationic fragment of the investigated ruthenium(II) ion pairs. Consequently, it was concluded that the overall ion pair rotation contributes mainly to the dipolar relaxation processes and that the determined interionic average distances were accurate. From such distances, it could also be concluded that in the case in which R = Me the aliphatic chain points away from the metal center. In fact, the distance between CH_2 and *o*H protons was about 0.7 Å shorter (Figure 9) than that relative to CH_2/B–Me protons; this is in perfect agreement with what was expected from molecular models.

AGGREGATION IN SOLUTION OF IONIC AND NEUTRAL NON-COVALENT INORGANIC COMPOUNDS

As illustrated in the section on PGSE measurements, PGSE NMR spectroscopy provides unique information for the characterization of non-covalent assemblies in solution in that it allows self-diffusion coefficients of molecules and their aggregates to be measured and, consequently, their size to be determined.

PGSE techniques are often applied to investigate non-covalently bonded organic systems. For example, Cohen et al.[72] have characterized multi-component hydrogen-bonded assemblies in solution and have demonstrated that the PGSE technique has sufficient resolution to distinguish between single, double, and tetrarosette assemblies. They also applied PGSE NMR to probe (1) the formation of self-assembled tetraurea calix[4]arene dimers in organic solvents via hydrogen bonds and (2) the encapsulation of guests in these "container molecules".[73] The application of PGSE studies to inorganic compounds is still limited.

Ionic Compounds

The association of organometallic ionic compounds as a function of solvent (chloroform-d and methylene chloride-d_2) and counteranion nature, $CF_3SO_3^-$, B, $(3,5\text{-}(CF_3)_2C_6H_3)_4^-$, and Cl^-, has been investigated through PGSE NMR measurements for some arene ruthenium(II) complexes bearing P,P-ligands by Pregosin et al.[74] In a recent interesting paper, the same authors showed that the field of application of PGSE measurements is not limited to nuclei with high receptivity (H and F) but can also be successfully applied to ^{31}P and ^{35}Cl nuclei.[75] This increases the counteranions that can be considered, i.e., ClO_4^-, $PO_4R_2^-$, etc.

By carrying out ^1H PGSE NMR studies on compounds **10**,[30a] in which M = Ru, we demonstrated that the type of ionic species present in solution is strongly affected by the solvent and concentration. As an example, ion quadruples are the predominant species in saturated solutions of *trans*-[Ru(COMe){$(pz_2)CH_2$}(CO)$(PMe_3)_2$]BPh_4(**A**) in chloroform-d while free ions are mainly present in nitromethane-d_3 solutions (Figure 10). These results can be deduced by comparing the slopes of the straight lines reported in Figure 10 relative to compound **A** and to *trans*-[Ru(COMe){$(pz_2)BH_2$}(CO)$(PMe_3)_2$](**B**) that is isosteric and almost isomass with the cation moiety of **A** ($\mathbf{A}^+$). **B** was used as an internal reference in order to be sure that the results were not affected by a change in the viscosity of the solutions. In case **a** of Figure 10 (chloroform-d), the ratio between the slopes (that corresponds to the ratio of the diffusion coefficients D_B/D_A) is equal to 1.6. By assuming **A** and **B** to be spherical, the volume ratio V_A/V_B is equal to 4.1 and, due to the fact that $\mathbf{A}^-$ and $\mathbf{A}^+$ have almost the same volumes, this ratio indicates

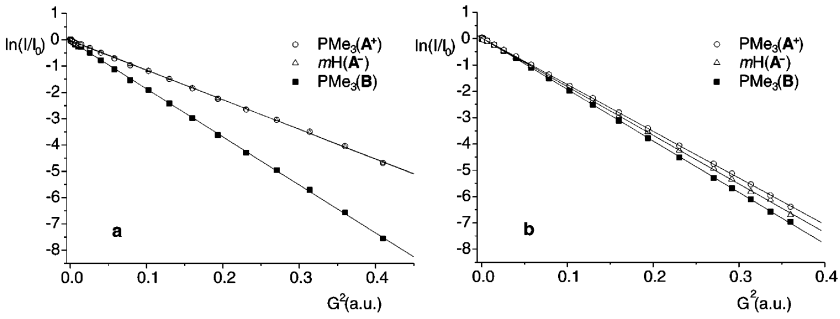

FIGURE 10 Plot of $\ln(I/I_0)$ versus G^2 (a.u. arbitrary units) for the PMe_3 resonances of $\mathbf{A}^+$ and **B** and for the *m*H resonance of $\mathbf{A}^-$ for the PGSE experiments carried out in (a) saturated solution of **A** in chloroform-d and (b) nitromethane-d_3 ($4 \cdot 10^{-3}$ M). Reproduced from Ref. 30a with the permission of the American Chemical Society.

that ion quadruples are mainly present in solution. On the other hand, the ratio of the slopes in case **b** (nitromethane-d_3) is 1.1 with a consequent volume ratio of 1.4 that can be explained with the main presence of free ions that have a volume a little higher than **B** due to the solvent that they drag during the translation. In between these two extreme cases, in which ion quadruples (**a**) or free ions (**b**) predominate, there is a continuum of situations corresponding to the simultaneous presence of ions, ion pairs and ion quadruples.

Several ionic organometallic compounds are active catalysts for reactions carried out in solvents with low dielectric constant and it is of fundamental importance to know if the species that really act as catalysts are free ions, ion pairs, ion quadruples, etc. Brintzinger et al.[76] tried to address this question by investigating zirconocene polymerization catalyst in the presence of boron-based cocatalysts in benzene-d_6 at 300 K. They concluded that, at least in some cases, ion quadruples are clearly present in solution. The lack of an internal standard and the known instability of the complexes in which the ion quadruples should be present leads to some perplexities. In a recent paper Babunskin and Brintzinger[32] estimated the size of the Me-MAO $^-$ anion by using an internal standard. The volume of the [Me-MAO] $^-$ anion suggests that it contains 150–200 Al atoms. In benzene solution the $[(C_5H_5)_2Zr(\mu\text{-Me})_2AlMe_2]^+$ [Me-MAO] $^-$ ion pair remains associated even at the lowest concentration studied and ion quadruples were appreciably present only at elevated concentration (0.012 M).

Neutral Compounds

The obvious difference between investigating neutral intermolecular adducts compared to ion pairs is the difficulty of having a reasonable percentage of intimate adducts in solution. The latter condition is fundamental, especially if one is interested in the relative orientation of the interacting units. We have started our investigations on intermolecular interactions by considering the possible stacking in solution of trinuclear cyclic basic Au(I) compounds $[Au(\mu\text{-}C^2,N^3\text{-bzim})]_3$ (bzim = 1-benzylimidazolate) (**13**) and $[Au(\mu\text{-C,N-C(OEt)=N–}C_6H_4\text{–}CH_3)]_3$ (**14**) with the trinuclear Hg(II) acid complex $[Hg(\mu\text{-C,C-}C_6F_4)]_3$ (**15**) (Scheme 6).[9]

While it is well-known that similar compounds stack in the solid state,[77] only indirect and inconclusive indications of the stacking process in solution have been reported. The $^{19}F,^1H$-HOESY NMR measurements showed the presence of intermolecular cross-peaks for solutions of both **13**/**15** and **14**/**15** adducts. In particular, intermolecular interactions were observed in **13**/**15** between F2 from **15**, and the CH_2, H4, H5 and *ortho*-protons from **13** (Figure 11). In adduct **14**/**15**, F2 interacts with the CH_2 protons of the OEt group and with the *ortho* protons. Thus we conclude that a reasonable

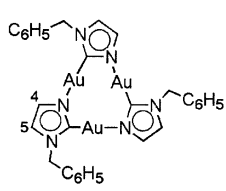

13

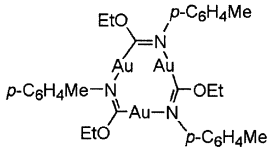

14

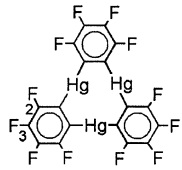

15

SCHEME 6

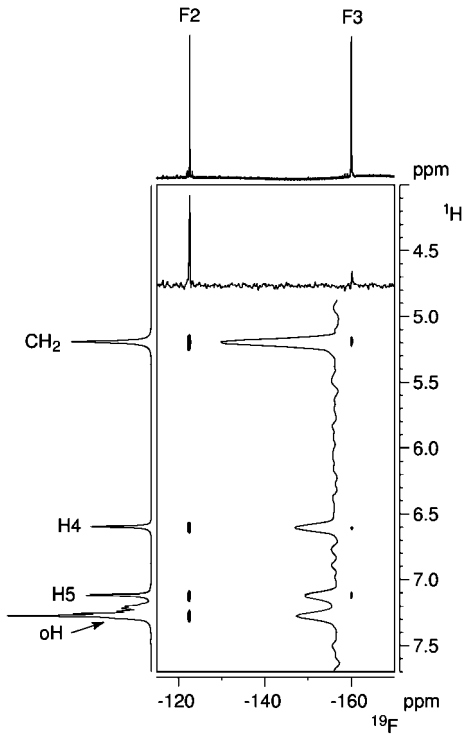

FIGURE 11 Section of a ^{19}F, ^{1}H-HOESY NMR spectrum of **13**/**15** adduct (9.6 mM in THF-d_8) at 376.63 MHz. Intermolecular NOEs are shown between F2 and the CH_2, H4, H5, and *o*H protons; and between F3 and the CH_2, H4, and H5 protons. The 1D-traces relative to the F2 column and CH_2 row are shown on the right and top of the section, respectively. Reproduced from Ref. 9 with the permission of the American Chemical Society.

percentage of intimate **13**/**15** and **14**/**15** adducts is present in solution. This represents the first direct evidence for supramolecular assembly in solution of **13**/**15** and **14**/**15**. These observations are consistent with the X-ray data, which show several short H–F distances (3.2–4.0 Å) for **13**/**15** and **14**/**15** adducts.[78] PGSE measurements allowed the size of the adducts to be quantified. There is an equilibrium between "Au_3Hg_3" and "$Au_3Hg_3Au_3$" aggregates for saturated solution of **13** and **15** complexes, while for **14** and **15** complexes, free molecules and "Au_3Hg_3" adduct are simultaneously present in solution.

CONCLUSIONS

The importance of NOE and PGSE NMR experiments stems from the fundamental role of weak interactions in determining the structure and reactivity of inorganic adducts in solution and the often-observed non-correspondence between the solid and solution structures.

The semi-quantitative NOE approach for determining the relative position of weakly bonded units has been successful. Unique information has been obtained about the interplay between anion-cation interactions and stoichiometric and catalytic reactivity of transition metal complex ion-pairs.[7] In addition, it has also provided a tool for estimating the steric hindrance that must be introduced in order to kinetically protect a metal center.[7,35,36] The applications regarding neutral inorganic adducts are still limited,[9] mainly because it is difficult to obtain a significant percentage of intimate adducts in solution.

The quantitative NOE approach, i.e., the estimation of the mean intermolecular distances, presents some difficulties due to the checks that must be done in order to be sure that the estimated distances are reasonably accurate. In any cases, it has been demonstrated that, once all the conditions have been satisfied, the average interionc distances can be estimated for transition metal complex ion pairs.[25]

Safe, interesting indications about the volumes of non-covalent aggregates in solution can be derived from PGSE NMR experiments. The latter seems to be widely applicable in that it can even be applied to multi-components systems and, in contrast to intermolecular NOE experiments, does not necessarily use nuclei with high receptivity.[77]

ACKNOWLEDGEMENT

This work was supported by grants from the Ministero dell'Istruzione, dell'Università e della Ricerca (MIUR, Rome, Italy), Programma di Rilevante Interesse Nazionale, Cofinanziamento 2002–2003.

REFERENCES

1. Müller-Dethlefs, K. and Hobza, P. 2000. Noncovalent interactions: A challenge for experiment and theory. *Chem. Rev.* 100, 143–167. Williams, D. H. and Westwell, M. S. 1998. Aspects of weak interactions. *Chem. Soc. Rev.* 27, 57–63.
2. Crabtree, R. H., Siegbahn, P. E. M., Eisenstein, O., Rheingold, A. L., and Koetzle, T. F. 1996. A new intermolecular interaction: Unconventional hydrogen bonds with element-hydride bonds as proton acceptor. *Acc. Chem. Res.* 29, 348–354. Custelcean, R. and Jackson, J. E. 2001. Dihydrogen bonding: Structures, energetics, and dynamics. *Chem. Rev.* 101, 1963–1980.
3. Braga, D., Grepioni, F., and Desiraju, G. R. 1998. Crystal engineering and organometallic architecture. *Chem. Rev.* 98, 1375–1406. Borovik, A. S. 2002. The use of non-covalent interactions in the assembly of metal/organic supramolecular arrays. *Comments Inorg. Chem.* 23, 45–78.
4. Mo, H. and Pochapsky, T. C. 1997. Intermolecular interactions characterized by nuclear overhauser effects. *Prog. NMR Spectrosc.* 30, 1–38.
5. Pochapsky, T. C. and Stone, P. M. 1990. Study of ion pair solution structure using nuclear Overhauser effects: interionic $^{1}H\{^{1}H\}$ and $^{11}B\{^{1}H\}$ NOEs in the $(CH_3CH_2CH_2CH_2)_4N^+$, BH_4^- ion pair. *J. Am. Chem. Soc.* 112, 6714–6715.
6. Bauer, W., Müller, G., Pi, R. and Schleyer, P. v. R. 1986. 2-Lithio-1-phenylpyrrole: X-ray structure analysis and ^{6}Li-^{1}H 2D heteronuclear Overhauser NMR spectroscopy (2D HOESY). *Angew. Chem. Int. Ed. Engl.* 25, 1103–1104. Avent, A. G., Eaborn, C., El-Kheli, M. N. A., Molla, M. E., Smith, J. D., and Sullivan, A. C. 1986. Utilization of the $^{6}Li\{^{1}H\}$ nuclear Overhauser effect. The structures of hydrido[tris(trimethylsilyl)methyl]metalates of boron, aluminum, gallium, and indium in solution. *J. Am. Chem. Soc.* 108, 3854–3855.
7. Macchioni, A. 2002. Elucidation of the solution structures of transition metal complex ion pairs by NOE NMR experiments. *Eur. J. Inorg. Chem.* 195–205.
8. Ribot, F., Sanchez, C., Willem, R., Martins, J. C. and Biesemans, M. 1998. Solution and solid state multinuclear NMR investigation of the Structure of $\{(BuSn)_{12}O_{14}(OH)_6\}(O_2PPh_2)_2$. *Inorg. Chem.* 37, 911–917.
9. Burini, A., Fackler, J. P. Jr., Galassi, R., Macchioni, A., Omary, M. A., Rawashdeh-Omary, M. A., Pietroni, B. R., Sabatini, S. and Zuccaccia, C. 2002. ^{19}F, ^{1}H-HOESY and PGSE NMR studies of neutral trinuclear complexes of Au^{I} and Hg^{II}: Evidence for acid-base stacking in solution. *J. Am. Chem. Soc.* 124, 4570–4571.
10. Stejskal, E. O. and Tanner, J. E. 1965. Spin diffusion measurements: Spin echoes in the presence of a time-dependent field gradient. *J. Chem Phys.* 42, 288–292. Stilbs, P. 1987. Fourier transform pulsed-gradient spin-echo studies of molecular diffusion. *Prog. in Nucl. Magn. Reson. Spectros.* 19, 1–45. Price, W. S. 1997. Pulsed-field gradient nuclear magnetic resonance as a tool for studying translational diffusion: Part 1. Basic theory. *Concepts Magn. Res.* 9, 299–336. Price, W. S. 1998. Pulsed-field gradient nuclear magnetic resonance as a tool for studying translational diffusion: Part II. Experimental aspects. *Concepts Magn. Res.* 10, 197–237. Johnson Jr., C. S. 1999. Diffusion ordered nuclear magnetic resonance spectroscopy: principles and applications. *Prog. Nucl. Magn. Res. Spectrosc.* 34, 203–256.
11. Noggle, J. H. and Schirmer, R. E. 1971. *The Nuclear Overhauser Effect*, New York: Academic Press.
12. The efficiency (or transition probability W) of a particular relaxation mechanism depends on the square of an interaction energy constant multiplied by a function of the correlation time (spectral density function):

$$W_{ij}=J(\omega)\left|\left(\langle i|\mathcal{H}_{\text{relaxation}}|j\rangle\right)^2\right|_{\text{average}} \qquad J(\omega)=\frac{2\tau_C}{1+\omega^2\tau_C^2}$$

13. Neuhaus, D. and Williamson, M. 2000. *The Nuclear Overhauser Effect in Structural and Conformational Analysis*, New York: WILEY-VCH, Chapters 2 and 3.
14. In real systems other relaxation mechanisms, different from dipole-dipole interaction, are active and, with the exception of relaxation coming from modulated scalar coupling, they only contribute to the single-quantum transition probabilities. As a consequence, the steady-state NOE can now be defined as $NOE_I\{S\} = \frac{\gamma_S}{\gamma_I}\frac{\sigma_{IS}}{\rho_{IS}+\rho^*_{IS}}$ where ρ^*_{IS} indicates the contribution to the total longitudinal relaxation rate coming from sources other than dipole-dipole interaction. In this case, the steady-state NOE for a two-spin system shows some distance dependence but its utility is limited because it is difficult to estimate the ρ^*_{IS} contribution.
15. When the assumption that $R_I = R_S = R$ breaks down, Equation 4 becomes somewhat more complicated. Similar mathematical approaches apply in the case of bidimensional experiments (namely NOESY or HOESY experiments).
16. The choice of the reference distance r_{AB} is critical in some respects and it is convenient that (a) A and B are not scalarly coupled, (b) r_{AB} is comparable to the "interesting distance," and (c) A and B do not undergo dynamic processes.
17. Lipari, G. and Szabo, A. 1982. Model-free approach to the interpretation of nuclear magnetic resonance relaxation in macromolecules. 1. Theory and range of validity. *J. Am. Chem. Soc.* 104, 4546–4559. Lipari, G. and Szabo, A. 1982. Model-free approach to the interpretation of nuclear magnetic resonance relaxation in macromolecules. 2. Analysis of experimental results. *J. Am. Chem. Soc.* 104, 4559–4570.
18. Tropp, J. 1980. Dipolar relaxation and nuclear Overhauser effects in nonrigid molecules: The effect of fluctuating internuclear distances. *J. Chem. Phys.* 72, 6035–6043.
19. Yip, P. F., Case, D. A., Hoch, J. C., Poulsen, F. M., Redfield, C., eds. 1991. *Computational Aspect of the Study of Biological Macromolecules by Nuclear Magnetic Resonance Spectroscopy*. New York: Plenum Press. pp. 317–330.
20. Olejniczak, E. T., Dobson, C. M., Karplus, M. and Levy, R. M. 1984. Motional averaging of proton nuclear Overhauser effects in proteins. Predictions from a molecular dynamics simulation of lysozyme. *J. Am. Chem. Soc.* 106, 1923–1930.
21. Post, C. B. J. 1992. Internal motional averaging and three-dimensional structure determination by nuclear magnetic resonance. *Mol. Biol.* 224, 1087–1101.
22. LeMaster, D. M., Kay, L.E., Brünger, A. T. and Prestegard, J. H. 1988. Protein dynamics and distance determination by NOE measurements. *FEBS Lett.* 236, 71–76.
23. Abseher, R., Lüdemann, S., Schreiber, H. and Steinhauser, O. 1994. Influence of molecular motion on the accuracy of NMR-derived distances. A molecular dynamics study of two solvated model peptides. *J. Am. Chem. Soc.* 116, 4006–4018.
24. Edmondson, S. P. 1994. Molecular dynamics simulation of the effects of methyl rotation and other protein motions on the NOE. *J. Magn. Reson. B.* 103, 222–233.
25. The rotational correlation time can be estimated by using both homonuclear and heteronuclear dipolar interactions; see, for example: Zuccaccia, C., Bellachioma, G., Cardaci, G. and Macchioni, A. 2001. Solution structure investigation of Ru(II) complex ion pairs: Quantitative NOE measurements and determination of average interionic distances. *J. Am. Chem. Soc.* 123, 11020–11028. In any case, it is common to consider the NOE measured distances as an estimation of the "real" distances, considering that the obtained values are generally affected by 5–10% error in accuracy.
26. Crank, J. 1975. *The Mathematics of Diffusion*, 2nd ed. Oxford: Clarendon Press. Einstein, A. 1956. *Investigations in the Theory of Brownian Movements*, New York: Dover. Callaghan,

P. T. 1975. *Principles of Nuclear Magnetic Resonance Microscopy*, Oxford: Oxford University Press.

27. This equation holds for perfect "stick boundary conditions"; other models were applied for the "slip boundary condition," in which the factor 6 must be replaced by 4: Robinson, R. A. and Stokes, R. H. 1970. *Elektrolyte Solutions*. London: Butterworth, 2nd ed., revised. Ue, M. 1994. Mobility and ionic association of lithium and quaternary ammonium salts in propylene carbonate and γ-butyrolactone. *J. Electrochem. Soc.* 141, 3336–3342. For large variations in the spherical shape, different friction factors must be taken into account. Cantor, C. R. and Schimmel, P. R. 1980. *Biophical Chemistry, Part II: Techniques for the Study of Biological Structure and Function*. San Francisco: W. H. Freeman.
28. Valentini, M., Rüegger, H., and Pregosin, P. S. 2001. Applications of pulsed-gradient spin echo (PGSE) diffusion measurement in organometallic chemistry. *Helv. Chim. Acta.* 84, 2833–2853.
29. Otting, G. and Wüthrich, K. 1990. Heteronuclear filters in two-dimensional [^{1}H,^{1}H]-NMR spectroscopy: Combined use with isotope labelling for studies of macromolecular conformation and intermolecular interactions. *Q. Rev. Biophys.* 23, 39–96.
30. (a) Zuccaccia, C., Bellachioma, G., Cardaci, G., and Macchioni, A. 2000. Self-diffusion coefficients of transition-metal complex ions, ion pairs, and higher aggregates by pulsed field gradient spin-echo NMR measurements. *Organometallics* 19, 4663–4665; (b) Mo, H. and Pochapsky, T. C. 1997. Self-diffusion coefficients of paired ions. *J. Phys. Chem. B.* 101, 4485–4486. (c) Valentini, M., Rüegger, H. and Pregosin, P. S. 2000. Applications of pulsed field gradient spin-echo measurements to the determination of molecular diffusion (and thus size) in organometallic chemistry. *Organometallics* 19, 2551–2556.
31. Jerschow, A. and Müller, N. J. 1997. Suppression of convection artifacts in stimulated-echo diffusion experiments. Double-stimulated-echo experiments. *Magn. Reson.* 125, 372–375.
32. Babushkin, D. E. and Brintzinger, H. H. 2002. Activation of dimethyl zirconocene by methylaluminoxane (MAO)-size estimate for Me-MAO anions by pulsed field-gradient NMR. *J. Am. Chem. Soc.* 124, 12869–12863.
33. van Koten, G. and Vrieze, K. 1982. 1,4-Diaza-1,3-butadiene (α-diimine) ligands: Their coordination modes and the reactivity of their metal complexes. *Adv. Organomet. Chem.* 21, 151–239.
34. Ittel, S. D., Johnson, L., and Brookhart, M. 2000. Late metal catalysts for ethylene homo- and copolymerization. *Chem. Rev.* 100, 1169–1203.
35. Bellachioma, G., Binotti, B., Cardaci, G., Carfagna, C., Macchioni, A., Sabatini, S., and Zuccaccia, C. 2002. Solution structure investigation of olefin Pd(II) and Pt(II) complex ion pairs bearing α-diimine ligands by ^{19}F, ^{1}H-HOESY NMR. *Inorg. Chim. Acta.* 330, 44–51.
36. Zuccaccia, C., Macchioni, A., Orabona, I. and Ruffo, F. 1999. Interionic solution structure of [PtMe(η^2-olefin)(N,N-diimine)]BF_4 complexes by ^{19}F{^{1}H}-HOESY NMR spectroscopy: Effect of the substituent on the accessibility of the counterion to the metal. *Organometallics* 18, 4367–4372.
37. Heiberg, H., Johansson, L., Gropen, O., Ryan, O. B., Swang, O. and Tilset, M. 2000. A combined experimental and density functional theory investigation of hydrocarbon activation at a cationic platinum(II) diimine aqua complex under mild conditions in a hydroxylic solvent. *J. Am. Chem. Soc.* 122, 10831–10845.
38. Bellachioma, G., Cardaci, G., D'Onofrio, F., Macchioni, A., Sabatini, S., and Zuccaccia, C. 2001. Interionic solution structure of acetyl Ru^{II} complexes bearing diimine and diamine ligands by ^{11}H-NOESY and ^{19}F{^{1}H}-HOESY NMR: Still more specific anion-cation interactions. *Eur. J. Inorg. Chem.* 1605–1611.

39. Fraser, L. C., Anastasi, N. R. and Lamba, J. J. S. 1997. Synthesis of halomethyl and other bipyridine derivatives by reaction of 4,4′-bis[(trimethylsilyl)methyl]-2,2′-bipyridine with electrophiles in the presence of fluoride ion. *J. Org. Chem.* 62, 9314–9317 and references therein.
40. Bianchini, C. and Meli, A. 2002. Alternating copolymerization of carbon monoxide and olefins by single-site metal catalysis. *Coord. Chem. Rev.* 225, 35–66.
41. Macchioni, A., Bellachioma, G., Cardaci, G., Travaglia, M., Zuccaccia, C., Milani, B., Corso, G., Zangrando, E., Mestroni, G., Carfagna, C. and Formica, M. 1999. Counterion effect on CO/styrene copolymerization catalyzed by cationic palladium(II) organometallic complexes: An interionic structural and dynamic investigation based on NMR spectroscopy. *Organometallics* 18, 3061–3069.
42. Romeo, R., Fenech, L., Monsù Scolaro, L., Albinati, A., Macchioni, A., and Zuccaccia, C. 2001. Fluxional behaviour of the dinitrogen ligand 2,9-dimethyl-1,10-phenantroline in cationic methyl platinum(II) complexes. *Inorg. Chem.* 40, 3293–3302.
43. Macchioni, A., Zuccaccia, C., Clot, E., Gruet, K. and Crabtree, R. H. 2001. Selective ion pairing in $[Ir(bipy)H_2(PRPh_2)_2]A$ ($A = PF_6$, BF_4, CF_3SO_3, BPh_4, $R = Me$, Ph): Experimental identification and theoretical understanding. *Organometallics* 20, 2367–2373.
44. Desmurs, P., Kavallieratos, K., Yao, W. and Crabtree, R. H. 1999. Intermolecular Re-H···H-N and Re-H···base hydrogen bonding estimated in solution by a UV-VIS spectroscopic method. *New. J. Chem.* 23, 1111–1115.
45. Reed, A. E., Weinstock, R. B., and Weinhold, F. 1985. Natural population analysis. *J. Chem. Phys.* 83, 735–746.
46. Drago, D., Pregosin, P. S, and Pfaltz, A. 2002. Selective anion effect in chiral complexes of iridium *via* diffusion and HOESY data: Relevance to catalysis. *Chem. Comm.* 286–287.
47. Trofimenko, S. 1993. Recent advances in poly(pyrazolyl)borate (scorpionate) chemistry. *Chem. Rev.* 93, 943–980.
48. Tsuji, S., Swenson, D. C., and Jordan, R. F. 1999. Neutral and cationic palladium(II) bis(pyrazolyl)methane complexes. *Organometallics* 18, 4758–4764. Byers, P. K. and Canty, A. J. 1990. Synthetic routes to methylpalladium (II) and dimethylpalladium (II) chemistry and the synthesis of new nitrogen donor ligand systems. *Organometallics* 9, 210–220.
49. Byers, P. K., Canty, A. J., Skelton, B. W. and White, A. H. 1990. Synthesis, reactivity, and structural studies in trimethylpalladium(IV) chemistry, including PdIMe3(bpy) and $[MMe_3((pz)_3CH)]^+$ (M = palladium, platinum). *Organometallics* 9, 826–832. Valk, J. M., Maassarani, F., van der Sluis, P., Spek, A. L., Boersma, J. and van Koten, G. 1994. Cyclopalladation of 2-[(dimethylamino)methyl]-substituted naphthalenes: 1- vs 3-palladation. Crystal structures of [hydrotris(pyrazolyl)borato][2-[(dimethylamino)methyl)]-3-naphthyl]palladium and trans-[4,4-dimethyl-2-(2-naphthyl)oxazoline]palladium dichloride. *Organometallics* 13, 2320–2329.
50. McWhinnie, W. R. 1970. Coordination behavior of some chelating ligands containing non- or weakly conjugated 2-pyridyl-groups. *Coord. Chem. Rev.* 5, 293–311.
51. Romeo, R., Arena, G., Monsù Scolaro, L., and Plutino, M. R. 1996. Rates of dimethyl sulfoxide exchange in monoalkyl cationic platinum(II) complexes containing nitrogen bidentate ligands. A Proton NMR Study. *Inorg. Chem.* 5, 293–311.
52. Binotti, B., Bellachioma, G., Cardaci, G., Macchioni, A., Zuccaccia, C., Foresti, E. and Sabatino, P. 2002. Intramolecular and interionic structural studies of novel olefin palladium(II) and platinum(II) complexes containing poly(pyrazol-1-yl)borate and -methane ligands. X-ray structures of palladium five-coordinate complexes. *Organometallics* 21, 346–354.

53. Romeo, R., Nastasi, N., Monsù Scolaro, L., Plutino, M. R., Albinati, A. and Macchioni, A. 1998. Molecular structure, acidic properties, and kinetic behavior of the cationic complex (methyl)(dimethyl sulfoxide)(bis-2-pyridylamine) platinum(II) Ion. *Inorg. Chem.* 37, 5460–5466.
54. Bellachioma, G., Cardaci, G., Macchioni, A., Reichenbach, G. and Terenzi, S. 1996. Application of ^{1}H-NOESY NMR spectroscopy to the investigation of ion pair solution structures of organometallic complexes by the detection of interionic contacts. *Organometallics* 15, 4349–4351.
55. Macchioni, A., Bellachioma, G., Cardaci, G., Gramlich, V., Rüegger, H., Terenzi, S. and Venanzi, L. M. 1997. Cationic bis- and tris(η^2-(pyrazol-1-yl)methane) acetyl complexes of iron(II) and ruthenium(II): Synthesis, characterization, reactivity, and interionic solution Structure by NOESY NMR spectroscopy. *Organometallics* 16, 2139–2145.
56. Macchioni, A., Bellachioma, G., Cardaci, G., Cruciani, G., Foresti, E., Sabatino, P. and Zuccaccia, C. 1998. Synthesis and structural studies of cationic bis- and tris(pyrazol-1-yl)methane acyl and methyl complexes of ruthenium(II): Localization of the counterion in solution by NOESY NMR spectroscopy. *Organometallics* 17, 5549–5556.
57. Schneider, H.-J., Schiestel, T. and Zimmermann, P. 1992. Host-guest supramolecular chemistry. 34. The incremental approach to noncovalent interactions: Coulomb and van der Waals effects in organic ion pairs. *J. Am. Chem. Soc.* 114, 7698–7703. Schneider, H.-J. 1994. Linear free energy relationships and pairwise interactions in supramolecular chemistry. *Chem. Soc. Rev.* 23, 227–234.
58. Lucet, D. L., Le Gall, T. and Mioskowski, C. 1998. The chemistry of vicinal diamines. *Angew. Chem. Int. Ed.* 37, 2580–2627.
59. Noyori, R. and Ohkuma, T. 2001. Asymmetric catalysis by architectural and functional molecular engineering: Practical chemo- and stereoselective hydrogenation of ketones. *Angew. Chem. Int. Ed.* 40, 40–73.
60. Slone, C. S., Weinberger, C. A. and Mirkin, C. A. 1999. *Progress in inorganic chemistry*. New York: Wiley. K. D. Karlin (ed.). 48: 233–350. Braunstein, P. and Naud, F. 1996. Hemilability of hybrid ligands and the coordination chemistry of oxazoline-based systems. *Angew. Chem. Int. Ed.* 40, 680–699.
61. Macchioni, A., Zuccaccia, C., Binotti, B., Carfagna, C., Foresti, E. and Sabatino, P. 2002. Cationic olefin Pd(II) complexes bearing α-iminoketone N,O-ligands: Unprecedented isomerisation of methoxycyclooctenyl ligand. *Inorg. Chem. Comm.* 5, 319–322.
62. Bellachioma, G., Cardaci, G., Gramlich, V., Macchioni, A., Valentini, M. and Zuccaccia, C. 1998. Cationic acetyl complexes of iron(II) and ruthenium(II) bearing neutral N,O ligands: Synthesis, characterization, and interionic solution structure by NOESY NMR spectroscopy. *Organometallics* 17, 5025–5030.
63. Zuccaccia, C., Bellachioma, G., Cardaci, G. and Macchioni, A. 1999. Specificity of Interionic contacts and estimation of average interionic distances by NOE NMR measurements in solution of cationic Ru(II) organometallic complexes bearing unsymmetrical counterions. *Organometallics* 18, 1–3.
64. Kessler, H., OschKinat, H., Griesinger, G. and Bermel, W. 1986. Trasformation of homonuclear two-dimensional NMR techniques into one-dimensional techniques using Gaussian pulses. *J. Magn. Res.* 70, 106–133.
65. Bauer, C. J., Freeman, R., Frenkiel, T., Keeler, J. and Shaka, J. 1984. Gaussian pulses. *J. Magn. Res.* 58, 442–457.
66. Stonehouse, J., Adel, P., Keeler, J. and Shaka, J. 1994. Ultrahigh-quality NOE spectra. *J. Am. Chem. Soc.* 116, 6037–6038.

67. Stott, K., Stonehouse, J., Keeler, J., Hwang, T.-L. and Shaka, J. 1995. Excitation sculpting in high-resolution nuclear magnetic resonance spectroscopy: Application to selective NOE experiments. *J. Am. Chem. Soc.* 117, 4199–4200.
68. Abragam, A. 1961. *The Principle of Nuclear Magnetism*, Oxford: Clarendon Press.
69. Bühl, M., Hopp, G., von Philipsborn, W., Beck, S., Prosenc, M.-H., Rief, U., and Brintzinger, H.-H. 1996. Zirconium-91 chemical shifts and line widths as indicators of coordination geometry distortions in zirconocene complexes. *Organometallics* 15, 778–785.
70. Gaemers, S., van Slageren, J., O'Connor, C. M., Vos, J. G., Hage, R. and Elsevier, C. J. 1999. ^{99}Ru NMR spectroscopy of organometallic and coordination complexes of ruthenium(II). *Organometallics* 18, 5238–5244.
71. Bellachioma, G., Cardaci, G., Gramlich, V., Macchioni, A., Pieroni, F. and Venanzi, L. M. 1998. Synthesis and characterisation of bis- and tris-(pyrazol-1-yl)borate acetyl complexes of Fe^{II} and Ru^{II} and isolation of an intermediate of B-N bond hydrolysis. *J. Chem. Soc., Dalton Trans.* 947–951.
72. Timmerman, P., Weidmann, J.-L., Jolliffe, K. A., Prins, L. J., Reinhoudt, D. N., Shinkai, S., Frish, L. and Cohen, Y. 2000. NMR diffusion spectroscopy for the characterization of multicomponent hydrogen-bonded assemblies in solution. *J. Chem. Soc., Dalton Trans.* 2077–2089.
73. Frish, L., Matthews, S. E., Böhmer, V. and Cohen, Y. 1999. A pulsed gradient spin echo NMR study of guest encapsulation by hydrogen-bonded tetraurea calix[4]arene dimers. *J. Chem. Soc., Perkin Trans.* 2, 669–671.
74. Valentini, M., Pregosin, P. S. and Rüegger, H. 2000. Applications of pulsed field gradient spin-echo measurements for the determination of molecular volumes of organometallic ionic complexes. *J. Chem. Soc., Dalton Trans.* 4507–4510.
75. Martinez-Viviente, E., Rüegger, H., Pregosin, P. S. and Lopez-Serrano, J. 2002. ^{31}P and ^{35}Cl PGSE diffusion studies on phosphine ligands and selected organometallic complexes. Solvent dependence of ion-pairing. *Organometallics* 21:5841–5846.
76. Beck, S., Geyer, A. and Brintzinger, H. H. 1999. Diffusion coefficients of zirconocene-borate ion pairs studied by pulsed field gradient NMR-evidence for ion quadruples in benzene solution. *Chem. Comm.* 2477–2478.
77. Burini, A., Fackler Jr., J. P., Galassi, R., Grant, T. A., Omary, M. A., Rawashdeh-Omary, M., Pietroni, B. R. and Staples, R. J. 2000. Supramolecular chain assemblies formed by interaction of a π-molecular acid complex of mercury with π-base trinuclear gold complexes. *J. Am. Chem. Soc.* 122, 11264–11265. Burini, A., Bravi, R., Fackler Jr., J. P., Galassi, R., Grant, T. A., Omary, M. A., Pietroni, B. R. and Staples, R. J. 2000. Luminescent chains formed from neutral, triangular gold complexes sandwiching Tl^{I} and Ag^{I}. Structures of $\{Ag([Au(\mu\text{-}C^2,N^3\text{-bzim})]_3)_2\}BF_4{\cdot}CH_2Cl_2$, $\{Tl([Au(\mu\text{-}C^2,N^3\text{-bzim})]_3)_2\}$-$PF_6{\cdot}0.5THF$ (bzim = 1-benzylimidazolate), and $\{Tl([Au(\mu\text{-}C(OEt){=}NC_6H_4CH_3)]_3)_2\}$-$PF_6{\cdot}THF$, with MAu_6 ($M = Ag^+$, Tl^+) cluster cores. *Inorg. Chem.* 39, 3158–3165 and references therein.
78. Burini, A., Fackler Jr., J. P., Galassi, R., Grant, T. A., Omary, M. A., Rawashdeh-Omary, M., Pietroni, B. R. and Staples, R. J. 2000. Supramolecular chain assemblies formed by interaction of a π molecular acid complex of mercury with π-base trinuclear gold complexes. *J. Am. Chem. Soc.* 122, 11264–11265.